ON THE USE OF MULTI-HARMONIC LEAST-SQUARES FITTING FOR THD ESTIMATION IN POWER QUALITY ANALYSIS

Pedro M. Ramos[1], Fernando M. Janeiro[2], Tomáš Radil[3]

1) Instituto de Telecomunicações, DEEC, Instituto Superior Técnico, Technical University of Lisbon, Av. Rovisco Pais 1,1049-001 Lisbon, Portugal (✉ pedro.m.ramos@ist.utl.pt, +351 21 841 8485)
2) Instituto de Telecomunicações, Universidade de Évora, Departamento de Física, Rua Romão Ramalho, n°. 59, 7000-671 Évora, Portugal (fmtj@uevora.pt)
3) Instituto de Telecomunicações, Av. Rovisco Pais 1, 1049-001 Lisbon, Portugal (tomas.radil@lx.it.pt)

Abstract

The quality of the supplied power by electricity utilities is regulated and of concern to the end user. Power quality disturbances include interruptions, sags, swells, transients and harmonic distortion. The instruments used to measure these disturbances have to satisfy minimum requirements set by international standards. In this paper, an analysis of multi-harmonic least-squares fitting algorithms applied to total harmonic distortion (THD) estimation is presented. The results from the different least-squares algorithms are compared with the results from the discrete Fourier transform (DFT) algorithm. The algorithms are assessed in the different testing states required by the standards.

Keywords: Harmonic analysis, Power quality, Signal reconstruction, Spectral analysis, Harmonic distortion.

1. Introduction

Power quality issues are of major concern to power producers, distributors and consumers [1]. Due to the increase in use of nonlinear loads, harmonic distortions are an ever increasing important issue in power quality analysis. While many of the typical disturbances that directly affect consumers are related with power outages (*i.e.*, interruptions), harmonic distortions can also cause major damages while not perceived by end users except when equipment fails. Traditionally, in measurements of power quality disturbances, the main strain on the measurement system is caused by the detection and classification of transients due to the required high sampling rate [2]. However, regulatory bodies are usually not concerned with transients, as Quality of Service (QoS) is mainly associated with RMS variations (*e.g.*, sags, swells, interruptions), frequency shifts, flicker, voltage unbalance and harmonic distortion. Therefore, a measurement device used for the assessment of quality of service must measure these parameters in real-time [3] and generate aggregate values according to the regulatory norms in effect in each country [4-6].

From the list of disturbances that must be assessed in quality of service related with power quality, the estimation of the harmonic component amplitudes and the total harmonic distortion (*THD*) is the most complex measurement [7]. For example, in IEC 61000-4-7 [4] for the Class I (equivalent to Class A in IEC 61000-4-30 [5]) the suggested method to determine the harmonic components is to estimate the FFT of the acquired signal and then estimate the individual amplitudes of the harmonic components to determine the *THD*. However, the estimation of the FFT requires a further strain on the acquisition system because it requires synchronous acquisition to ensure that any frequency variations do not cause spectral leakage and errors in the estimation of the harmonic amplitudes and on the final *THD*

value [8]. In [9] an efficient alternative to the use of coherent sampling was proposed for active power estimation, based on windowing. Time-frequency algorithms such as the Gabor-Wigner Transform (GWT) have also been proposed for power quality assessment [10].

This paper describes the DSP implementation of an alternative method for the estimation of the harmonic amplitudes and *THD* value that does not require synchronous acquisition. The method is based on least-squares fitting of the acquired samples [11]. The outputs of this method are the harmonic amplitudes, the harmonic phases (not directly relevant for the assessment of power quality harmonic distortions) and the *THD*. As a by-product, the use of this algorithm enables the estimation of a new parameter called total interharmonic distortion (*TIHD*) which accounts for the distortion present in the signal that does not correspond to harmonic distortion. This new parameter is estimated by removing, from the initially acquired signal, the signal reconstructed from the estimated harmonics (using the amplitudes and phases of each harmonic) and then estimating the RMS value of these residuals. This parameter enables the detection of events caused by non-harmonics of the fundamental signal.

This paper includes a detailed description of the algorithm and also of the details required for implementation in a DSP-based standalone QoS measurement system. Extensive tests of the proposed algorithm will demonstrate its compliance with the uncertainty limits set in IEC 61000-4-30 in the three testing states which include other disturbances besides harmonic distortions (namely frequency variations, flicker, voltage amplitude variations and presence of interharmonics). The standard IEC 61000-4-30 requires that, in these three test states and with the presence of the other disturbances, the harmonic evaluation must remain within certain boundaries for each specific harmonic. The accuracy requirements depend on the Class of instrument: Class I of the IEC 61000–4–7 corresponds to Class A of IEC 61000–4–30, while Class II of the IEC 61000–4–7 corresponds to Class S of IEC 61000–4–30. The requirements are based on the relation between the magnitudes of the measured harmonics and the nominal voltage range.

In the end, the decision to implement a specific algorithm in a standalone DSP-based measurement system [12, 13] depends on the suitability of the algorithm to estimate the desired parameter (in this case the harmonic amplitudes and the *THD*), on the speed with which the algorithm can be executed (of particular importance for real-time systems such as power quality QoS assessment) and the amount of memory the algorithm requires (crucial in standalone measurement systems where memory is scarce and an expensive add-on that can also slow down algorithm execution).

2. Power quality standard and harmonic estimation

In this section, an overview of the standards that specify the conditions for power metering instrument testing is presented. The IEEE 1159 standard [6] classifies harmonics in an electric power system as the steady-state waveform distortions that are in the range 0 Hz to 9 kHz with a magnitude up to 20% of the fundamental. The general instrument used to measure harmonic distortion is described in standard IEC 61000-4-7 [4]. Although the standard proposes a DFT-based instrument, it allows the use of different algorithms. Measurement methods in power quality parameters are defined in IEC 61000-4-30 [5] which requires that at least 50 harmonics are estimated.

The accuracy requirements for harmonic estimation are defined in standard 61000-4-7 and are divided into two classes: Class I and Class II. The classes correspond to different accuracy requirements in the relation between the magnitude of the measured harmonics u_h and the nominal voltage range u_{nom}. A third class of instruments, (Class B in IEC 61000-4-30), is also defined for instruments whose performance is defined by the manufacturer. The accuracy requirements for Class I and Class II are shown in Table 1.

Standard IEC 61000-4-30 specifies the measuring range using the compatibility levels defined in standard IEC 61000-2-4 [14] for low-frequency disturbances in industrial environments. The compatibility levels depend on the maximum disturbance levels that a device may be subjected to. For Class A devices the measuring range should be from 10% to 200% of the Class 3 compatibility levels defined in IEC 61000-2-4, while for the less-accurate Class S it should be from 10% to 100% of the same Class 3 levels. These Class 3 compatibility levels are shown in Table 2. The compatibility levels for odd harmonics are higher than those for the even harmonics, as it is usual in power systems to have dominant odd harmonics. This standard also defines that, for class 3, the maximum total harmonic distortion is 10%.

Table 1. Accuracy requirements for Class I and Class II voltage harmonics measurement.

Class	Condition	Maximum Error
I	$u_h \geq 1\% \, u_{nom}$	$\pm 5\% \, u_h$
	$u_h < 1\% \, u_{nom}$	$\pm 0.05\% \, u_{nom}$
II	$u_h \geq 3\% \, u_{nom}$	$\pm 5\% \, u_h$
	$u_h < 3\% \, u_{nom}$	$\pm 0.15\% \, u_{nom}$

Table 2. Voltage harmonics compatibility levels defined in IEC 61000-2-4 for Class 3.

Harmonic order h	Class 3 compatibility level % of fundamental	Harmonic order h	Class 3 compatibility level % of fundamental
2	3	11	5
3	6	13	4.5
4	1.5	15	2
5	8	17	4
6	1	21	1.75
7	7	$10 < h \leq 50$ (h even)	1
8	1	$21 < h \leq 45$ (h odd multiples of three)	1
9	2.5		
10	1	$17 < h \leq 49$ (h odd)	$4.5 \cdot (17/h) - 0.5$

The test signals used in the classification of the measurement instruments should include other disturbances besides the harmonic content. Three testing states are defined in IEC 61000-4-30 corresponding to different levels of disturbances. The conditions for each testing state are described in Table 3. The nominal power frequency is f_{nom} and P_{st} is the short-term flicker severity.

Table 3. IEC 61000-4-30 testing state conditions for Class A and Class S instruments.

Quantity	Testing State 1	Testing State 2	Testing State 3
Frequency	$f_{nom} \pm 0.5 \, \text{Hz}$	$f_{nom} - 1 \, \text{Hz} \pm 0.5 \, \text{Hz}$	$f_{nom} + 1 \, \text{Hz} \pm 0.5 \, \text{Hz}$
Flicker	$P_{st} < 0.1$	$P_{st} = 1 \pm 0.1$	$P_{st} = 4 \pm 0.1$
Voltage	$u_{nom} \pm 1\%$	Determined by flicker and interhamonics	Determined by flicker and interhamonics
Inter-harmonics	0% to 0.5% of u_{nom}	$1\% \pm 0.5\%$ of u_{nom} at $7.5 f_{nom}$	$1\% \pm 0.5\%$ of u_{nom} at $3.5 f_{nom}$

3. Least-squares fitting algorithms

In this section, the least-squares fitting algorithms are described and their use for the estimation of the total harmonic distortion is detailed. In [15] and [16], two basic sine-fitting

algorithms were standardized for ADC and waveform records testing. These algorithms are not multi-harmonic in the sense that they only estimate the parameters of the fundamental. Multi-harmonic versions of the sine-fitting algorithms were developed in [11] and improved in [17]. These algorithms were successfully used in impedance measurements [18, 19].

Modern power quality analyzers are based on acquisition systems where an analog-to-digital converter (ADC) is used to sample the voltage sensor output at a given sampling rate (for 3-phase systems there is one ADC for each phase). Typically a digital signal processor (DSP) retrieves the digital output of the ADC samples and algorithms implemented in the DSP are then used to estimate the desired parameters of the acquired signal (for example, frequency, RMS value, average value, harmonic amplitudes and total harmonic distortion). Specifically for the estimation of the harmonic distortion, it is usual to consider that the distortion is of a steady-state nature in the sense that the causes of harmonic distortion are not completely random in nature and that the duration of such distortions largely exceeds the period of the acquired signal. Therefore, the acquired signal is modeled by

$$u(t) = C + \sum_{h=1}^{H} \left[A_h \cos(2\pi f h t) + B_h \sin(2\pi f h t) \right] + u_\varepsilon(t) = C + \sum_{h=1}^{H} \left[D_h \cos(2\pi f h t + \varphi_h) \right] + u_\varepsilon(t) \quad (1)$$

where C is the DC component, f is the signal frequency, H is the number of harmonics considered in the model, A_h is the in-phase amplitude of harmonic h, B_h is the in-quadrature amplitude of harmonic h, D_h is the amplitude of harmonic h, φ_h is the phase of harmonic h and $u_\varepsilon(t)$ accounts for the residuals of the model (which will include higher harmonics, interharmonics, noise and other disturbances such as transients). The signal fundamental corresponds to $h=1$ while the harmonics correspond to $h>1$. Ideally, all the harmonics should have zero amplitude.

Note that both representations in (1) are equivalent and related by

$$D_h = \sqrt{A_h^2 + B_h^2} \qquad \varphi_h = -\operatorname{atan} 2(B_h, A_h) \qquad (2)$$

or reciprocally by $A_h = D_h \cos(\varphi_h)$ and $B_h = -D_h \sin(\varphi_h)$.

The Total Harmonic Distortion (*THD*) is an indicator used to express the total amount of harmonic components. It is defined as the ratio between the RMS of the harmonics and the RMS of the fundamental

$$THD = \sqrt{\sum_{h=2}^{H} \left(\frac{D_h}{D_1} \right)^2}. \qquad (3)$$

The *THD* is usually expressed in relative units or in percentage. The use of logarithmic units (dB) is usually limited to the analysis of distortion in linear systems where distortion is much smaller than in power systems.

For stationary signals whose length is exactly 10 cycles for 50 Hz power systems or 12 in case of 60 Hz power systems, the whole energy of a harmonic component is concentrated in one frequency bin of the FFT (*i.e.*, there is no spectral leakage). However, if the signal's parameters change such as its fundamental frequency, the energy will leak into nearby frequency bins due to spectral leakage. To take into account this effect, standard IEC 61000-4-7 defines two more indicators: the group total harmonic distortion (*THDG*) and the subgroup total harmonic distortion (*THDS*).

The group total harmonic distortion is defined as

$$THDG = \sqrt{\sum_{h=2}^{H}\left(\frac{U_{g,h}}{U_{g,1}}\right)^2} \text{ , where } U_{g,h}^2 = \frac{U^2\left[P \times h - \frac{P}{2}\right]}{2} + \sum_{k=-\frac{P}{2}+1}^{\frac{P}{2}-1} U^2\left[P \times h - k\right] + \frac{U^2\left[P \times h + \frac{P}{2}\right]}{2}, \quad (4)$$

where P is the number of periods in the acquisition segment and $U[k]$ is the amplitude of each individual frequency component obtained from the *FFT*.

The subgroup total harmonic distortion is defined as

$$THDS = \sqrt{\sum_{h=2}^{H}\left(\frac{U_{sg,h}}{U_{sg,1}}\right)^2} \text{ , where } U_{sg,h}^2 = \sum_{k=-1}^{1} U^2\left[P \times h + k\right], \quad (5)$$

meaning that the RMS value of each harmonic is obtained from the three FFT elements closer to the ideal harmonic frequency. Note that these two parameters are solely defined and of relevance to enable the use of the FFT under spectral leakage conditions. The use of least-squares fitting directly estimates the harmonic amplitudes and is immune to spectral leakage since it does not require the use of the FFT.

The Total InterHarmonic Distortion (*TIHD*) is an indicator used to express the total value of RMS not associated with the fundamental or the harmonics in the acquired signal

$$TIHD = \sqrt{\frac{1}{N}\sum_{n=1}^{N} u_\varepsilon^2[n]}, \quad (6)$$

where N is the number of samples in the acquisition segment and $u_\varepsilon[n]$ is the residual associated with sample n.

In the following subsections the four basic least-squares algorithms are presented. Their use to estimate the *THD* will be addressed in Section 4.

3.1. Three-parameter sine-fitting

The three-parameter sine-fitting estimates three parameters of the signal model: the in-phase amplitude, the in-quadrature amplitude and the DC component. It requires the knowledge of the signal frequency and it is a multiple linear regression. The estimated parameters **x** are obtained from

$$\mathbf{x} = \begin{bmatrix} C & A_1 & B_1 \end{bmatrix}^T = \begin{bmatrix} \mathbf{D}^T\mathbf{D} \end{bmatrix}^{-1}\mathbf{D}^T\mathbf{u} \text{ with } \mathbf{D} = \begin{bmatrix} \mathbf{1} & \mathbf{c}_1 & \mathbf{s}_1 \end{bmatrix}, \quad (7)$$

where **u** is the vector with the N samples and **1** is a vector with N rows all equal to 1, $\mathbf{c}_h = \cos(2\pi hf\mathbf{t})$, $\mathbf{s}_h = \sin(2\pi hf\mathbf{t})$ and **t** is the N rows vector with the timestamps corresponding to each sample.

This algorithm is not iterative and therefore it is quite straightforward to be used. However, due to the fact that the frequency is not estimated and that the frequency in power systems can change, it is not actually suited for direct use in the assessment of the harmonic amplitudes. To also estimate the signal frequency, the four-parameter sine-fitting should be used.

If the DC component is not required, the algorithm can be adapted by removing the first element of vector **x** and the first column of matrix **D**. This modification does not change the estimation results.

3.2. Four-parameter sine-fitting

The four-parameter sine-fitting is iterative (due to the fact that the frequency must also be estimated, it is no longer a multiple linear regression) and the estimated parameters in iteration i are $\mathbf{x}^{(i)} = \begin{bmatrix} C & A_1 & B_1 & \Delta\omega^{(i)} \end{bmatrix}^T$ where $\Delta\omega^{(i)}$ is the angular frequency correction in iteration i which is used to update the estimated angular frequency correction of the previous iteration with $\omega^{(i)} = 2\pi f^{(i)} = \omega^{(i-1)} + \Delta\omega^{(i)}$. The estimated parameters are obtained with $\mathbf{D} = \begin{bmatrix} \mathbf{1} & \mathbf{c}_1 & \mathbf{s}_1 & \boldsymbol{\alpha}_1 \end{bmatrix}$ where $\boldsymbol{\alpha}_h = -A_h^{(i-1)} h(\mathbf{t} \circ \mathbf{s}_h) + B_h^{(i-1)} h(\mathbf{t} \circ \mathbf{c}_h)$ ($\circ$ is the Hadamard product or entrywise product). Note that $\mathbf{D}$ must be recalculated in each iteration because the frequency changes and the amplitudes estimated in the previous iteration are used to determine $\boldsymbol{\alpha}_h$. The criterion to detect convergence is to stop the iterations when the absolute relative frequency correction is below a threshold, *i.e.*, when $\left| \Delta\omega^{(i)} / \omega^{(i)} \right| < \varepsilon_\omega = 10^{-7}$.

In this algorithm it is crucial to begin with the best estimated values for the frequency and amplitudes. If improper estimations are used, the algorithm may require many iterations to converge or even fail to converge. To ensure a reduced number of iterations, the initial frequency estimation is usually obtained from the IpDFT [20] and the in-phase and in-quadrature amplitudes are obtained from the three-parameter sine-fitting algorithm (using the IpDFT estimated signal frequency). By complying with these basic rules, the number of iterations is typically below 5.

3.3. Non-iterative multi-harmonic fitting

The non-iterative multi-harmonic fitting can estimate the amplitudes of the harmonics for a given frequency. The $2H+1$ estimated parameters are $\mathbf{x} = \begin{bmatrix} C & A_1 & B_1 & A_2 & B_2 & \cdots & A_H & B_H \end{bmatrix}^T$ which are obtained from $\mathbf{x} = \begin{bmatrix} \mathbf{D}^T \mathbf{D} \end{bmatrix}^{-1} \mathbf{D}^T \mathbf{u}$ with $\mathbf{D} = \begin{bmatrix} \mathbf{1} & \mathbf{c}_1 & \mathbf{s}_1 & \mathbf{c}_2 & \mathbf{s}_2 & \cdots & \mathbf{c}_H & \mathbf{s}_H \end{bmatrix}$. Note that $\mathbf{D}$ has N rows and $2H+1$ columns. The elements of $\mathbf{x}$ can be used to estimate the *THD* using (2) and (3). If the DC component is not required, the algorithm can also be adapted by removing the first element of $\mathbf{x}$ and the first column of $\mathbf{D}$ without changing the *THD* estimation results.

3.4. Iterative multi-harmonic fitting

The iterative multi-harmonic fitting also estimates the signal frequency much like the four-parameter sine-fitting algorithm. The $2H+2$ estimated parameters are $\mathbf{x} = \begin{bmatrix} C & A_1 & B_1 & A_2 & B_2 & \cdots & A_H & B_H & \Delta\omega^{(i)} \end{bmatrix}^T$ and $\mathbf{D} = \begin{bmatrix} \mathbf{1} & \mathbf{c}_1 & \mathbf{s}_1 & \mathbf{c}_2 & \mathbf{s}_2 & \cdots & \mathbf{c}_H & \mathbf{s}_H & \sum_{h=1}^{H} \boldsymbol{\alpha}_h \end{bmatrix}$.

Obviously, this is the most direct algorithm to estimate the *THD* but it comes with a cost both memory-wise and computationally.

4. Use of least-squares fitting algorithms for THD estimation

Three different options to use the least-squares fitting algorithms for *THD* estimation are presented in this section. In all situations, the outcome is the harmonic amplitudes, their phases, the fundamental frequency and the DC component. Then, the *THD* is directly obtained from (3) while *TIHD* can be obtained from (6) using the residuals of the fit.

www.czasopisma.pan.pl PAN www.journals.pan.pl
POLSKA AKADEMIA NAUK

Metrol. Meas. Syst., Vol. XIX (2012), No. 2, pp. 295-306.

The first option is to use the four-parameter sine-fitting on the acquired signal to estimate the signal frequency, the DC component and the fundamental parameters. The residuals of this fit are then applied to the three-parameter sine-fitting (without DC component) to estimate the parameters of the second harmonic (h=2) and so on until all the harmonics are estimated. The main drawbacks of this method are that the errors of the signal frequency are propagated into the harmonics and the need to estimate the residuals is an added computational burden.

The second option is to apply the four-parameter sine-fitting to obtain the frequency and parameters of the fundamental and then apply the non-iterative multi-harmonic fitting to its residuals. This estimates, in one step, the parameters of all harmonics and reduces the computational burden of estimating the residuals of the three-parameter sine-fitting for each harmonic. The drawback is caused by the fact that the frequency is estimated in the first step and its errors are accumulated in the multi-harmonic fit. Another disadvantage is the fact that the burden of the multi-harmonic fit is considerably higher than that of the three-parameter sine-fitting. However, since the multi-harmonic is applied only once and the three-parameter fitting must be applied to each harmonic, the overall computational burden must be assessed.

The third option is to use solely the iterative multi-harmonic fitting. This option is straightforward but it is the most demanding, computationally and memory-wise.

5. Developed power quality analyzer

In this section, the developed power quality analyzer is described. Different sensor modules are available using a wide selection of ranges (namely for the current). Each of these modules can be used to interface the power system and the acquisition and processing module. In addition there is one module responsible for power management which includes a backup rechargeable Li-Ion battery to power the system in case of sags and interruptions. When power is restored the battery is recharged. If the battery is totally drained during a longer interruption, the system shuts down and restarts when power is restored.

The acquisition and processing module includes some analog signal conditioning for each channel (from the current and voltage sensors), one 16-bit analog to digital converter (ADC) per channel, a memory module to add storage capacity during processing and one digital signal processor where the samples are processed and the algorithms are implemented. The system block diagram is presented in Fig. 1.
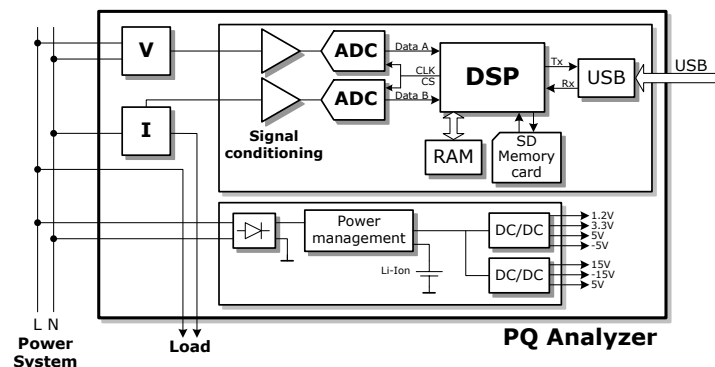

Fig. 1. Basic block diagram of the implemented PQ analyzer.

The system can be interfaced by a SD memory card or a USB connection. Basically these interfaces are used to store the detected events and monitor in real time the operation of the PQ analyzer. The acquisition itself is controlled by the DSP which sets the sampling rate of the ADCs to 50 kS/s. Each acquisition segment lasts 3 s which corresponds to 150 000

samples. DMA is used to transfer the acquired samples, during the segment acquisition, into the external memory. While one segment is being acquired, the previous segment must be completely processed by the DSP. Although this paper is focused on the estimation of the total harmonic distortion, in DSP all the algorithms for detection of events are implemented. In Fig. 2, the complete block diagram of the algorithms is presented.

After a pre-processing stage, the algorithms are divided into two sections. In the lower section of Fig. 2, the RMS values are estimated and thresholds are used to determine if an event was detected and if so, the classification stage determines its amplitude, duration and type (sag, swell, overvoltage, undervoltage or interruption) from the RMS values [21].
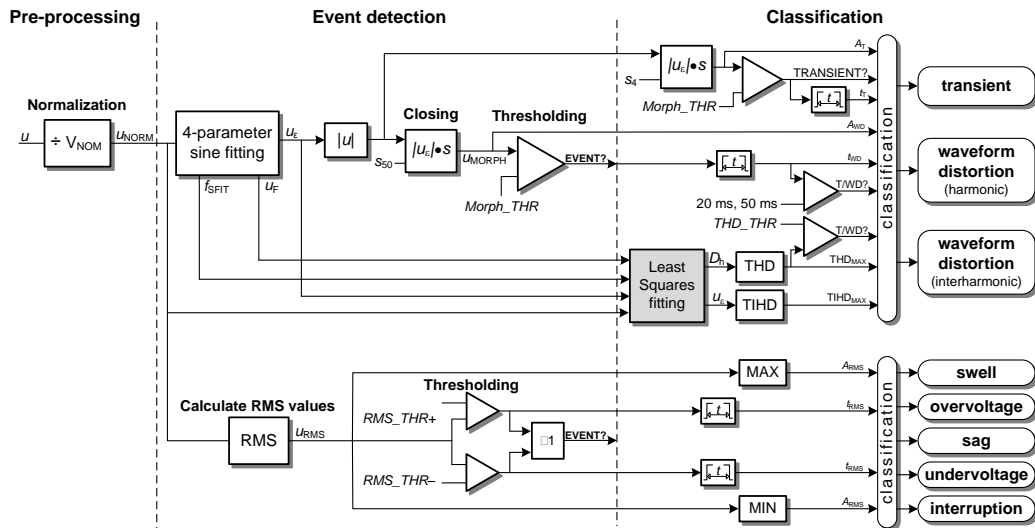
Fig. 2. Block diagram of the algorithms implemented in the PQ analyzer.

The second section deals with the detection of transients and waveform distortions. Here, the first algorithm to be applied is the four-parameter sine-fitting to separate the fundamental from the rest of the signal (the residuals include harmonics, interharmonics, transients and noise). To estimate if an event is present in the current segment, the morphological operation closing [22, 23] is used with a structuring element of length equivalent to 50 ms. With this operation, thresholding is then a straightforward operation to detect if an event is present since it groups multiple crossings of the threshold for a single event. The duration of the event, as estimated from the closing operation, is then used to assess which class of event occurred. If the event duration is above 50 ms or if it is above 20 ms and the *THD* exceeds the *THD* threshold, then it is a waveform distortion (either caused by *THD* − harmonic distortion − or *TIHD* − interharmonic waveform distortion). If this condition is not verified, then the event is a transient and another morphological closing operation is applied with a smaller structuring element (equivalent to 4 ms) to separate transients that might be close to each other in the residuals and also to estimate with better accuracy the duration of the transient.

The evaluation of the *THD* and *TIHD* is done using one of the algorithms defined in section IV in the gray block of Fig. 2. Notice, however, that the 4-parameter sine-fitting has already been applied and therefore the burden is reduced in the first two cases, while in the third case the full algorithm of the iterative multi-harmonic sine-fitting must nevertheless be applied.

6. Results

Fig. 3 depicts an acquired waveform (50 Hz nominal frequency) with some clear harmonic distortion near the zero crossings of the rising edge of the sine signal. Also visible but less

discernable are some harmonic distortions near the signal peaks. This is a clear example of a power voltage distorted by the presence of non-linear loads. In Fig. 3, the amplitude units (pu) correspond to the traditional normalization with respect to the nominal RMS value of the distribution voltage. This normalization is useful when comparing systems with different nominal RMS voltages and is widely used in PQ.
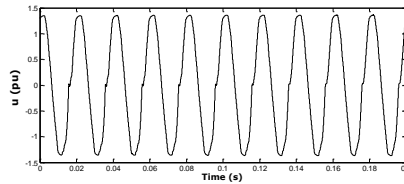

Fig. 3. Example of distorted voltage signal in a power system.

Since for Class A instruments, the measuring range is up to 200%, the harmonic amplitudes can reach twice the values of the harmonic levels of Table 2. Nevertheless, the maximum total harmonic distortion is 20% and if all the harmonics have their maximum value, the *THD* would exceed this limit value. Therefore, the signal used for testing can have harmonic amplitudes up to twice those of Table 2 but making sure that the *THD* does not exceed 20%. In Table 4, the harmonic amplitudes of the test signals are presented. They represent a compromise between the maximum amplitude of the harmonics and the desired *THD* value. With these values, the *THD* is 20%.

Table 4. Harmonic content of the test signal.

Harmonic order h	Harmonic amplitude in % of fundamental
2	4
3	12
4	2
5	10
7	4
$9 \leq h \leq 17$ (h odd)	2
$6 \leq h \leq 18$ (h even)	1.6
$19 \leq h \leq 50$	1.6

For the harmonic amplitudes presented in Table 4, the maximum allowed error for each harmonic for Class I and Class II (from Table 1) is presented in Fig. 4. Notice that, for the higher order harmonics, their amplitude is much lower and therefore, the maximum error is a percentage of the nominal system voltage and does not depend on the harmonic amplitudes themselves. For all the testing states, the signals contained white Gaussian noise with 75 dB SNR. For each state, 10 000 signals were tested and the maximum error of individual harmonics amplitudes were registered.
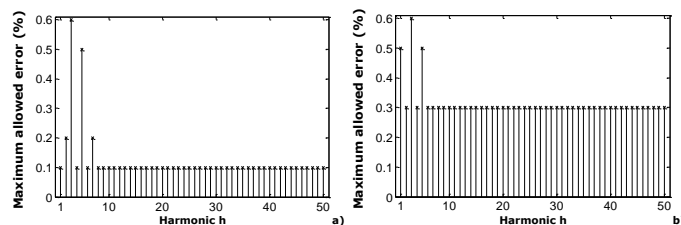

Fig. 4. Maximum allowed error in the estimation of each harmonic for the test signal with the harmonic content shown in Table 4 for: a) Class I instruments; b) Class II instruments.

6.1. Testing State 1

In this testing state, relatively low flicker is applied, as well as low amplitude interharmonics, the frequency is centered on the nominal value and the nominal voltage can

change by 1%. The results obtained with the four algorithms are presented in Fig. 5 – the DFT results are also included for comparison. It can be seen that almost all algorithms comply with the requirements for Class A. The combined four-parameter and three-parameter sine-fitting algorithm only complies with Class S.
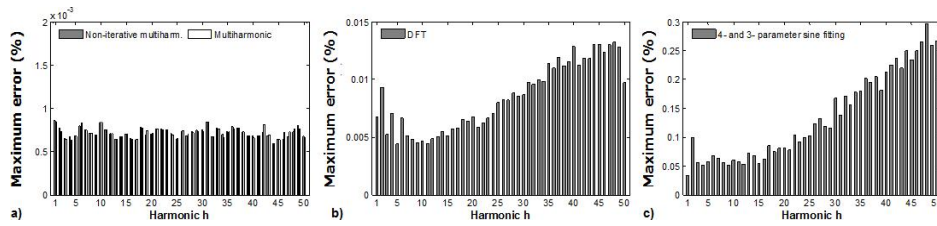

Fig. 5. Accuracy in the harmonic amplitude estimation in testing state 1.

6.2. Testing State 2

In testing state 2 the frequency is centered 1 Hz below the nominal value with some small variation and a moderate amount of flicker is included. A moderate-valued interharmonic is added at frequency $7.5f_{nom}$.

The results in this testing state are presented in Fig. 6 and it can be seen that both iterative and noniterative multi-harmonic algorithms satisfy the minimum requirements for instruments of both Class A and Class S. The combined four-parameter and three-parameter sine-fitting algorithm only complies with the requirements for Class S instruments as its maximum error at higher order harmonics is just below 0.3% and well above 0.1%. Notice that the results obtained in this testing state are similar to the ones obtained in testing state 1.
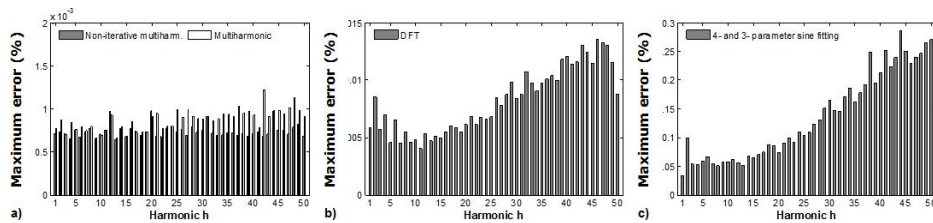

Fig. 6. Accuracy in the harmonic amplitude estimation in testing state 2.

6.3. Testing State 3

In the third testing state, the frequency is centered 1 Hz above its nominal value with some small variation and a severe amount of flicker is included in the signal. The included interharmonic has a moderate amplitude and is located at $3.5\,f_{nom}$. Fig. 7 shows the results for this testing state with all the algorithms, including the DFT for comparison. Once again both multi-harmonic algorithms are fully compliant with the requirements for both instrument classes and perform better than the DFT algorithm. The combined four-parameter and three-parameter sine-fitting algorithm again only complies with Class S instruments. The maximum error results for all the tested algorithms are similar in all testing states.
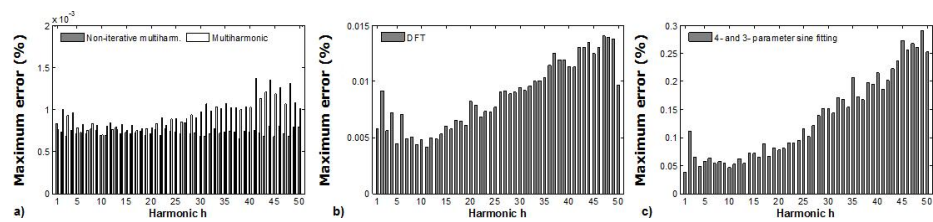

Fig. 7. Accuracy in the harmonic amplitude estimation in testing state 3.

6.4. THD estimation comparison

In Fig. 8, a comparison of the maximum error obtained when estimating the *THD* value with the different algorithms an as a function of the applied *THD* is presented for testing state 3. It can be seen that the worst results are obtained for the *THDG* method for *THD* values below 5% (caused by the interharmonics influencing the computation of *THDG* according to (4)) and that for higher distortions, the worst algorithm is again the combined four-parameter and three-parameter sine-fitting algorithm.
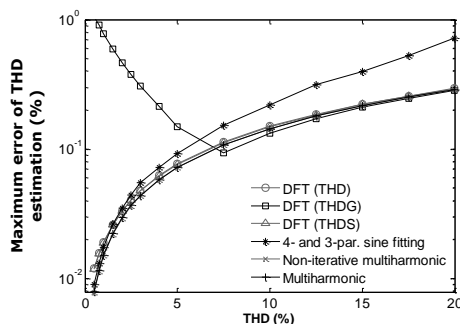

Fig. 8. Comparison of the *THD* accuracy for the tested algorithms in testing state 3.

7. Conclusions

In this paper a detailed comparison of least-squares fitting algorithms for *THD* estimation for power quality analyzers is presented. There are three options that can be used with the main difference being the computational complexity and burden of the algorithms. One of the presented solutions (the combined four-parameter and three-parameter sine-fitting algorithm) is only viable for Class S instruments which correspond to instruments used for statistical applications such as surveys or power quality assessment. For Class A instruments (used when precise measurements are required) either multi-harmonic algorithm may be used.

It should be noted that the computational burden of these algorithms puts added pressure on DSP-based systems. To reduce the computational burden of the least-squares fitting algorithms, decimation can be applied to the complete set of acquired samples. This is a valid approach because the maximum harmonic to be assessed should be near 9 kHz and the sampling rate is much higher (50 kS/s). Therefore if only one sample in each 2 is used, the sampling rate would be reduced to 25 kS/s which would still be enough to estimate harmonics up to 9 kHz. If only 50 harmonics are needed, the decimation factor can be increased and the computational burden further reduced. Note that the decimation should be applied only before the Least Squares fitting block of Fig. 2 but that the complete acquired signal must be used for the four-parameter sine-fitting to estimate transients.

The developed system (described in Fig. 1 and Fig. 2) is capable of monitoring, in real-time, the power quality of a single-phase power system. It includes data logging capabilities and an internal backup power source to sustain operation during interruptions and sags. The system has been used to generate a database of real recorded power quality events which is available online for the use of the scientific community working in power quality.

References

[1]   Dugan, R.C., McGranaghan, M.F., Santoso, S., Beaty, H.W.(2003). *Electrical Power Systems Quality*. NY: McGraw-Hill, 2nd edition.

[2] Radil, T., Ramos, P.M., Janeiro, F.M., Serra, A.C. (2008). PQ monitoring system for real-time detection and classification of disturbances in a single-phase power system. *IEEE Trans. Instrum. Meas.*, 57(8), 1725-1733.

[3] Ardeleanu, A.S., Ramos, P.M. (2011). Real time PC implementation of power quality monitoring system based on multiharmonic least-squares fitting. *Metrol. Meas. Syst.*, 18(4), 543-554.

[4] IEC 61000-4-7 Electromagnetic compatibility (EMC) – Part 4-7: Testing and measurement techniques – General guide on harmonics and interharmonics measurements and instrumentation, for power supply systems and equipment connected thereto, Edition 2.1, IEC, 2009.

[5] IEC 61000-4-30 Electromagnetic compatibility (EMC) – Part 4-30: Testing and measurement techniques – Power quality measurement methods, Edition 2.0, 2008.

[6] IEEE Std. 1159-2009. IEEE Recommended Practice for Monitoring Electric Power Quality. *IEEE Power & Energy Society*, 2009.

[7] Tarasiuk, T., Mindykowski, J. (2012). An extended interpretation of THD concept in the wake of ship electric power systems research. *Measurement*, 45(2), 207-212.

[8] Bollen, M.H.J., Gu, I.Y.H.(2006). *Signal Processing of Power Quality Disturbances*. NJ: Wiley.

[9] Sedlacek, M., Stoudek, Z. (2011). Active power measurements - an overview and comparison of DSP algorithms by noncoherent sampling. *Metrol. Meas. Syst.*, 18(2), 173-184.

[10] Szmajda, M., Górecki, K., Mroczka, J. (2010). Gabor Transform, SPWVD, Gabor-Wigner Transform and Wavelet Transform - Tools for Power Quality monitoring. *Metrol. Meas. Syst.*, 17(3), 383-396.

[11] Ramos, P.M., Silva, M.F., Martins, R.C., Serra, A.C. (2006). Simulation and experimental results of multiharmonic least-squares fitting algorithms applied to periodic signals. *IEEE Trans. Instrum. Meas.*, 55(2), 646-651.

[12] Radil, T., Janeiro, F.M., Ramos, P.M., Serra, A.C. (2008). An efficient approach to detect and classify power quality disturbances. *International Journal for Computation and Mathematics in Electrical and Electronic Engineering (COMPEL)*, 27(5), 1178-1191.

[13] Radil, T., Ramos, P.M., Serra, A.C. (2009). Single-phase power quality analyzer based on a new detection and classification algorithm. In *Procedings of IMEKO World Congress*. Lisbon, Portugal, 917-922.

[14] IEC 61000-2-4 Electromagnetic compatibility (EMC) – Part 2-4: Environment – Compatibility levels in industrial plants for low-frequency conducted disturbances, Edition 2, IEC, 2002.

[15] IEEE Std. 1057-2007, IEEE Standard for Digitizing Waveform Recorders, New York, April 2008.

[16] IEEE Std. 1241-2011, IEEE Standard for Terminology and Test Methods for Analog-to-Digital Converters, New York, 2011.

[17] Ramos, P.R., Serra, A.C. (2007). Least Squares Multiharmonic fitting: Convergence improvements. *IEEE Trans. Instrum. Meas.*, 56(4), 1412-1418.

[18] Ramos, P.R., Serra, A.C. (2008). Impedance measurement using multiharmonic least-squares waveform fitting algorithm. *Computer Standards and Interfaces, Elsevier*, 30(5), 323-328.

[19] Janeiro, F.M., Ramos, P.M. (2009). Impedance measurements using genetic algorithms and multiharmonic signals. *IEEE Trans. Instrum. Meas.*, 58(2), 383-388.

[20] Renders, H., Schoukens, J., Vilain, G. (1984). High-accuracy spectrum analysis of sampled discrete frequency signals by analytical leakage compensation. *IEEE Trans. Instrum. Meas.*, 33(4), 287-292.

[21] Styvaktakis, E., Bollen, M.H.J., Gu, I.Y.H. (2002). Automatic classification of power system events using RMS voltage measurements. *IEEE Power Engineering Society Summer Meeting*, 824-829.

[22] Serra, J. (1982). *Image Analysis and Mathematical Morphology*, 1. Academic Press.

[23] Radil, T., Ramos, P.M., Janeiro, F.M., Serra, A.C. (2007). DSP Based Power Quality Analyzer for Detection and Classification of Disturbances in a Single-phase Power System. *Metrol. Meas. Syst.*, 14(4), 483-494.